

## Fragrance-containing microcapsules based on interfacial thiol-ene polymerization

Ziyang Liao,<sup>1</sup> Daquan Xue,<sup>2</sup> Hao Li,<sup>1</sup> Lei Shi<sup>3</sup>

<sup>1</sup>School of Pharmacy, East China University of Science and Technology, Shanghai 200237, China

<sup>2</sup>Shanghai Yilian Chemical and Hi-Tech Co., Ltd., Shanghai 201203, China

<sup>3</sup>Corporate R&D Division, Firmenich Aromatics (China) Co., Ltd., Shanghai 201108, China

Correspondence to: H. Li (E-mail: hli77@ecust.edu.cn) and L. Shi (E-mail: lei.rocky.shi@firmenich.com)

**ABSTRACT:** In this study, microcapsules containing fragrance oils as active agent were synthesized by interfacial thiol-ene polymerization in oil-in-water emulsion. One water-soluble dithiol and four oil-soluble acrylates were used as “click”able monomers. The polymerization kinetics was studied by HPLC and <sup>1</sup>H-NMR. The size and morphology of the microcapsules were characterized by means of light scattering, optical microscope, and scanning electron microscope, and their thermal property was examined by TGA. The encapsulation efficiency and stability of the microcapsules were monitored at room temperature and 45 °C for 1 month. In general, this interfacial thiol-ene polymerization was demonstrated to be a facile and efficient approach for fragrance microencapsulation with new and stable shell materials. © 2016 Wiley Periodicals, Inc. *J. Appl. Polym. Sci.* **2016**, *133*, 43905.

**KEYWORDS:** applications; kinetics; membranes

Received 8 March 2016; accepted 10 May 2016

DOI: 10.1002/app.43905

### INTRODUCTION

Fragrances are used in numerous personal and household care products such as detergents, fabric softeners, shampoos, and shower gels to enhance the products' olfactory appeal or to mask undesired odors.<sup>1</sup> Sustained release of fragrances is a key performance parameter of those products. However, most fragrance materials are highly volatile, and their aroma is rapidly lost on application. Meanwhile, because of the existence of reactive functional groups, many fragrance molecules are susceptible to environmental elements including water, oxygen, heat, and light and may cause serious stability issues, for example, deteriorating olfactory profile and color change.<sup>2</sup> To overcome these limitations, one representative solution is to encapsulate the fragrance inside a solid matrix.<sup>3</sup> Besides protecting fragrances and controlling the release, encapsulation can also serve to promote other desired properties such as efficient deposition of fragrances toward target surfaces.<sup>4–6</sup> Among the existing encapsulation systems, polymeric microcapsules synthesized via interfacial polymerization are widely used. In interfacial polymerization, oil-in-water (O/W) or water-in-oil (W/O) emulsion is prepared with oil-soluble monomers and water-soluble monomers dissolved in oil and water phases, respectively, and then the monomers react at the oil–water interface to form a polymeric shell.<sup>7,8</sup> In the industry, the majority of commercial fragrance microcapsules consists of poly(urea–formaldehyde), poly(melamine–

formaldehyde), polyurethane, or polyurethane–urea shell materials because of their superior thermal and mechanical properties and readily available and cheap monomers.<sup>9–12</sup> However, to minimize the amount of residual monomers including isocyanate, melamine, and formaldehyde, prolonged reaction time, elevated temperature, and scavenger molecules are frequently required and lead to higher cost.<sup>13</sup> Therefore, exploring new types of chemistry with improved feasibility and reaction efficiency for the development of polymeric microcapsules is of fundamental importance in fragrance applications.

On the other hand, since the introduction by Sharpless and coworkers in 2001,<sup>14</sup> click chemistry, because of its remarkable advantages (e.g., simple reaction conditions, high efficiency and orthogonality, and tolerance to functional groups), has been extensively used in many research fields including fabrication of functional polymeric materials.<sup>15–20</sup> In particular, over the past few years, several click chemistry-based strategies have been reported for the synthesis and modification of polymeric capsules. For example, copper(I)-catalyzed azide–alkyne cycloaddition (CuAAC) was used by De Geest et al. to form hydrogel microcapsules with alkyne- and azide-functionalized dextrans as monomers.<sup>21–23</sup> Bernard and coworkers<sup>24</sup> synthesized nanocapsules by CuAAC interfacial step-growth polymerization in mini-emulsion conditions. With the assistance of microwave irradiation, the reaction finished in 30 min with 98%

conversion rate. By using electron-deficient alkynes, Landfester and coworkers<sup>25</sup> also developed copper-free azide–alkyne interfacial polymerization for preparing nanocapsules. Moreover, CuAAC-type crosslinking can be used in combination with layer-by-layer assembly to prepare microcapsules.<sup>26–29</sup> In addition to azide–alkyne cycloaddition, another type of click chemistry, thiol–ene photopolymerization was also reported by Cheng and coworkers<sup>30</sup> to prepare nanocapsules with dithiol monomers crosslinking allyl-functionalized PEO-*b*-PLA copolymers in the oil phase. However, to the best of our knowledge, until now there are few reports on using click chemistry in interfacial polymerization for the synthesis of capsules in micron size regime. Although nanocapsules are of high fundamental research interest, such carriers have difficulty in encapsulating volatile actives with high stability because of their ultrathin membrane structure. In addition, to entrap same quantity of oil, nanocapsules require larger amount of emulsifier and more energy input to prepare, and thus, they are less cost effective than microcapsules. For these reasons, microcapsules are preferred for fragrance applications. Herein, we use water-soluble dithiol and oil-soluble acrylate as “click”able monomers for interfacial thiol–ene polymerization to fabricate fragrance-containing microcapsules. The polymerization kinetics was studied by HPLC and <sup>1</sup>H-NMR. The size and morphology of the microcapsules were characterized by means of light scattering, optical microscope, and scanning electron microscope, and their thermal property was examined by TGA. The encapsulation efficiency (EE) and stability of the microcapsules were monitored at room temperature and 45 °C for 1 month.

## EXPERIMENTAL

### Materials

Trimethylolpropane triacrylate (A1) and pentaerythritol tetraacrylate (A2) were received from Energy Chemical and Thermo-Fisher, respectively. Dipentaerythritol pentaacrylate (A3) and dipentaerythritol hexaacrylate (A4) were obtained from Sigma-Aldrich as a mixture and were isolated using a silica gel column. Mowiol 18-88 was also obtained from Sigma-Aldrich. DL-1,4-Dithiothreitol (D1), phenol, and isooctane were purchased from Adamas Reagent. Nile red (Nanjing BioDuly Chemicals) was used as tracer, and K<sub>2</sub>CO<sub>3</sub> (Wuxi Jiani Chemistry) was used as catalyst. A model fragrance oil was prepared by mixing four ingredients: cyclosal [3-(4-isopropylphenyl)-2-methylpropanal], romascone (methyl 2,2-dimethyl-6-methylenecyclohexanecarboxylate), verdox (*o*-*tert*-butylcyclohexyl acetate), and dorisyl (*p*-*tert*-butylcyclohexyl acetate), which were provided by Firmenich, at equal mass percentage. Acetonitrile (Fulltime Reagent), diethyl ether (Shanghai Lingfeng Reagent), and CDCl<sub>3</sub> and D<sub>2</sub>O (Cambridge Isotope Laboratories) were used as solvents. Except A3 and A4, all reagents and solvents were used as received without further purification.

### Nuclear Magnetic Resonance Spectroscopy

<sup>1</sup>H-NMR and <sup>13</sup>C-NMR spectra were acquired on a Bruker Ascend 400 MHz NMR spectrometer.

A3 <sup>1</sup>H-NMR (400 MHz, CDCl<sub>3</sub>, δ): 6.44–6.38 (m, 5H), 6.15–6.08 (m, 5H), 5.89–5.85 (m, 5H), 4.27 (s, 6H), 4.21 (s, 4H), 3.60 (s, 2H), 3.45 (s, 4H); <sup>13</sup>C-NMR (100 MHz, CDCl<sub>3</sub>, δ):

165.99, 165.62, 131.66, 131.46, 127.88, 127.72, 70.16, 69.68, 62.75, 62.68, 61.32, 44.74, 43.33.

A4 <sup>1</sup>H-NMR (400 MHz, CDCl<sub>3</sub>, δ): 6.40 (d, *J* = 17.2, 6H), 6.13–6.06 (m, 6H), 5.86 (d, *J* = 10.4, 6H), 4.24 (s, 12H), 3.49 (s, 4H); <sup>13</sup>C-NMR (100 MHz, CDCl<sub>3</sub>, δ): 165.52, 131.49, 127.78, 70.05, 62.76, 43.15.

### Preparation of Microcapsules by Interfacial Polymerization

Interfacial polymerization was done by following a typical procedure reported in the literature.<sup>31</sup> An acrylate monomer (A1–A4) was dissolved in 15 g of the model fragrance oil, and the mixture was stirred for 15 min to form a homogeneous oil phase. About 45 g stock solution of Mowiol 18-88 (2%) was weighed as the aqueous phase. The two phases were homogenized for 3 min using an Ultra-Turrax T25 disperser at 10,000 rpm to form the O/W emulsion. Then, the O/W emulsion was moved to a 200-mL reactor and stirred with a mechanical overhead stirrer. The water-soluble monomer (D1) and 0.04 g of the catalyst (K<sub>2</sub>CO<sub>3</sub>) dissolved in 12 g of deionized water were added dropwise to the stirring mixture with a syringe. The total amount of monomers was ~0.85 g, and the molar feed ratio was as follows: D1/A1 = 2.25/1, D1/A2 = 3/1, D1/A3 = 3.75/1, and D1/A4 = 4.5/1. The reaction was stopped after 3 h of stirring, and the resulting suspension was collected in a 100-mL beaker.

### Particle Size and Morphology Characterization

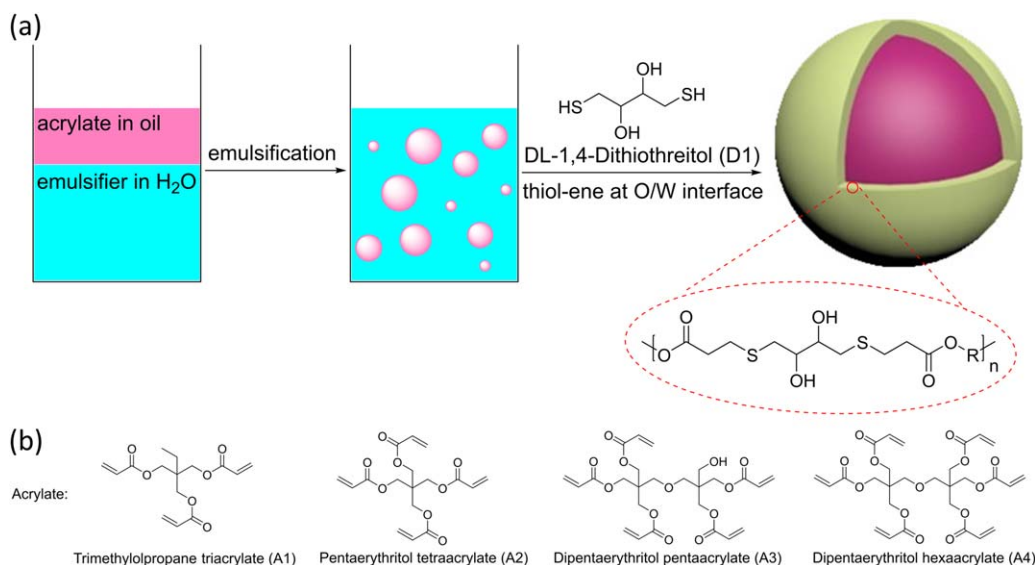
Size distributions were measured at room temperature via light scattering under Fraunhofer model using a Malvern Mastersizer 3000 equipped with a Hydro LV sample dispersion unit. Optical images were taken on a Nikon Eclipse Ci optical microscope, and scanning electron microscopy (SEM) images were obtained on a JEOL JSM-6360LV SEM.

### Study of Reaction Kinetics

At set time intervals after the injection of D1 and K<sub>2</sub>CO<sub>3</sub>, 1.0 g of the reaction mixture was taken to a centrifuge tube, and 2.0 g of deionized water was added for dilution. The diluted suspension was centrifuged at 4000 rpm for 1 min, and the supernatant aqueous phase was removed. This water washing was repeated once, and the slurry layer was dispersed in 2.5 mL of acetonitrile, shaken on a vortex mixer for 2 min, and centrifuged at 4000 rpm for 1 min. The supernatant liquid was filtered using 0.22-μm membrane filter and then analyzed by HPLC. HPLC was done on a Shimadzu LC-20A equipped with Shim-pack GIS C18 column using gradient elution of acetonitrile in water (from 10 to 90% in 25 min) at 25 °C. For select reaction (D1A1), the supernatant aqueous phase was collected after the washing, frozen, and lyophilized to dryness. The solid residue was redissolved in D<sub>2</sub>O that contained 20 mg/mL phenol as internal standard and examined by <sup>1</sup>H-NMR.

### Determination of Encapsulation Efficiency of Microcapsules

About 2.5 g of the microcapsule suspension was weighed in a vial, and then 1 g of deionized water and 1 mL of extractant (isooctane/ethyl ether = 90/10, v/v) were added. The mixture was shaken on an incubator shaker for 2 min to extract the nonencapsulated fragrance and was centrifuged at 4000 rpm for 2 min. About 400 μL of the supernatant was transferred to a preweighed



**Scheme 1.** (a) Interfacial thiol-ene polymerization process toward microcapsules. (b) Structures of the acrylate monomers used (A1–A4). [Color figure can be viewed in the online issue, which is available at [wileyonlinelibrary.com](http://wileyonlinelibrary.com).]

round-bottomed flask. The organic solvent was removed under reduced pressure, and the oil collected was weighed to quantify the amount of extracted oil. Each measurement was performed in triplicate. The leakage of the model oil was checked by measuring the EE of the microcapsules stored at room temperature and 45 °C. The samples were taken to repeat the above procedure at 1 week and 1 month after the tests started.

#### Thermogravimetric Analysis of Microcapsules

Thermogravimetric analysis was performed on a TA Instruments TGA Q500. An aliquot of microcapsule suspension was analyzed in nitrogen atmosphere with a purge rate of 60 mL/min. For each microcapsule, two temperature programs were tested: ramp 5 °C/min to 50 °C and isothermally hold for 4 h; and ramp 5 °C/min to 300 °C and isothermally hold for 1 h. Data were processed using TA Universal Analysis software.

## RESULTS AND DISCUSSION

### Microcapsule Formation

Scheme 1 illustrates the interfacial thiol-ene polymerization process. Four oil-soluble monomers (A1–A4) with electron-deficient C=C bonds (acrylate) were selected to react with the water-soluble monomer D1. All these monomers are commercially available. Prior to the thiol-ene reaction, the model fragrance oil containing an acrylate monomer was emulsified with polyvinyl alcohol (Mowiol 18-88) as nonionic emulsifier and stabilizer under mild homogenization conditions (10,000 rpm for 3 min). Consequently, an O/W emulsion could be produced with polydisperse droplet size ranging from submicron to tens of micron [Figure 1(a)]. Based on the light scattering results [Figure 2(a)], the A3-based emulsion had a volume-average diameter ( $D[4,3]$ ) of 15.7  $\mu\text{m}$ . When the reaction was stopped 3 h after the addition of D1 and  $\text{K}_2\text{CO}_3$  solution, optical microscope [Figure 1(b)] and light scattering [Figure 2(a)] found that the microcapsule size ( $D[4,3] = 19.7 \mu\text{m}$ ) was slightly bigger than the emulsion droplet. The oil encapsulation was also clearly visualized when a lipophilic dye, Nile red, was dissolved

in the model oil (0.15% relative to the oil phase). Changing the oil-soluble monomer from A1 to A4 has only a marginal effect on the final capsule size [Figure 2(a,b)]. Figure 1(b,c) also shows that the microcapsules produced by this method were generally in spherical shape, and no significant aggregated particles were found. In pilot-scale production, aggregation should be avoided as it might lead to very large particles that require extra steps to remove. Thus, the production of discrete particles in laboratory suggested a lower risk of aggregation when scaled up. Figure 1(d,e) shows the morphology of microcapsule D1A4 when viewed by SEM. The microcapsules appeared to have a rather rough surface; dense convex spots of a few hundred nanometers size and some areas of wrinkling spread all over the shell surface.

### Reaction Kinetics of Interfacial Thiol-ene Polymerization

All thiol-ene polymerizations were run under base catalysis at room temperature. In interfacial polymerization, to construct the polymeric membrane, usually the water-soluble monomer diffuses toward the oil side of the interface, where the polymerization occurs.<sup>32</sup> Therefore, D1 was used in excess relative to the acrylate monomers, and the molar feed ratio was maintained in a way such that thiol group (–SH)/acrylate group (–OCOCH<sub>2</sub>) = 1.5/1. The reactions were monitored through HPLC by quantifying the oil-soluble monomers at set time intervals such as the one displayed in Figure 3(a) for A1. The conversion ratios of A1–A4 were plotted against time in Figure 3(b). It can be seen that for A1 and A2, around 40% monomer was consumed in the first 10 min after the D1 and  $\text{K}_2\text{CO}_3$  addition, and the reaction was almost finished in less than 30 min. Although the reaction of A3 seemed slower, it was finished after 40 min. By sharp contrast, only 13 and 24% A4 was found reacted at 10 and 30 min, and even after the reaction had been allowed to continue for a whole day, there was 10% A4 remaining unreacted. This result indicates that the polymerization is highly dependent on the characteristics of the acrylate

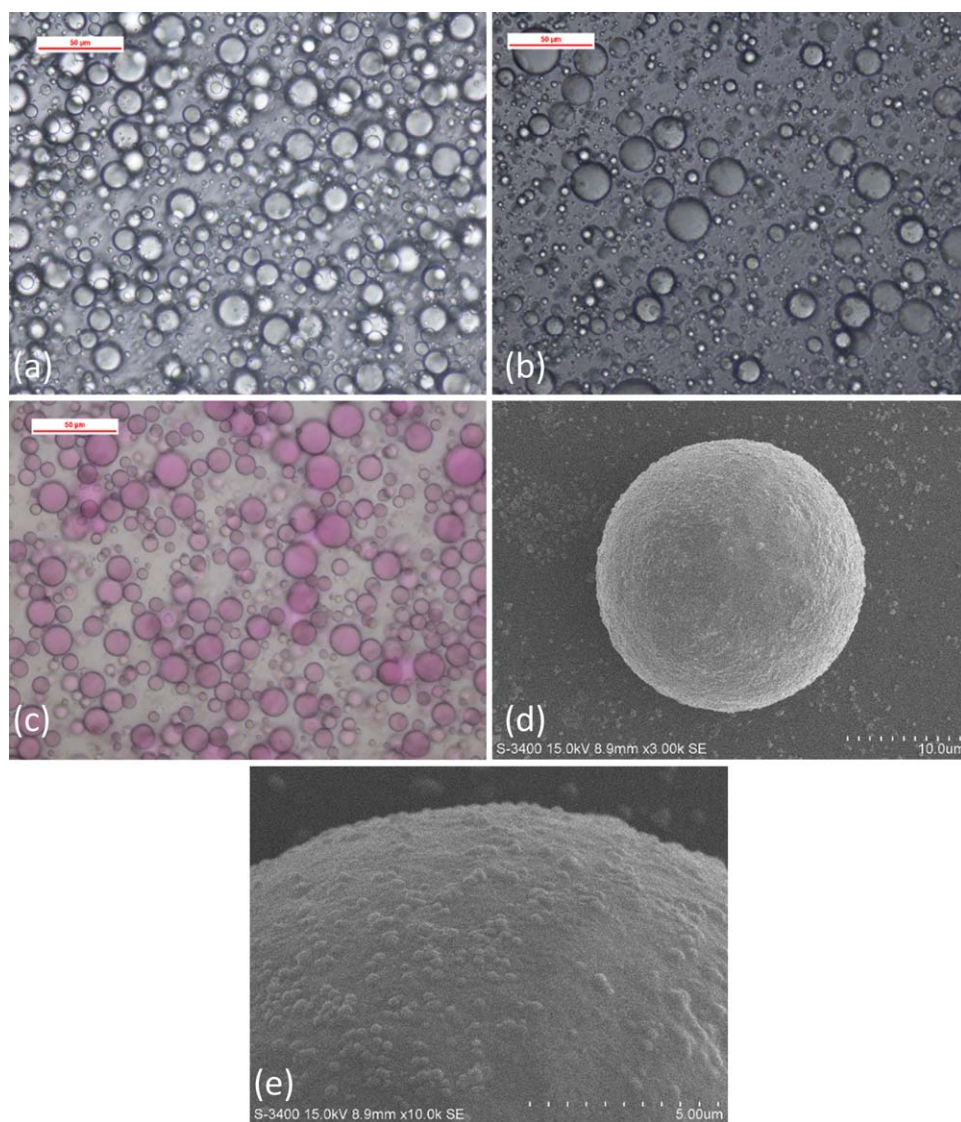


**Figure 1.** Optical microscopic images of (a) A3 O/W emulsion, (b) D1A3 capsules synthesized via interfacial thiol-ene polymerization, and (c) D1A2 capsules synthesized with 0.15% Nile red in oil phase. SEM images of single D1A4 capsule at magnification (d)  $\times 3000$  and (e)  $\times 10,000$ . [Color figure can be viewed in the online issue, which is available at [wileyonlinelibrary.com](http://wileyonlinelibrary.com).]

monomers used. It is speculated that as the polymerization started, D1 crossed the interfacial barrier from the aqueous phase into the oil phase to react with the acrylate monomer which was soon depleted in the thin reaction zone. With the reaction zone occupied by oligomers and polymers formed, it consequently become less lipophilic and more sterically hindered. According to the calculated  $\log P$  values from Advanced Chemistry Development (ACD/Labs), A4 is clearly more hydrophobic than the other three acrylates: 2.674 (A1), 2.186 (A2), 2.645 (A3), and 3.463 (A4). Therefore, the diffusion of A4 into the reaction zone might be hampered by the larger molecular size and more hydrophobic nature of A4, whereas A1–A3 did not exhibit a sign of such rate-limiting step.

In addition to HPLC, the reaction between D1 and A1 was selected to monitor the D1 concentration by  $^1\text{H-NMR}$ . As shown in Figure 3(c), the peaks located at  $\delta = 3.60$  and 2.55 ppm were assigned to the methine and methylene protons

of D1. The intensity of these two signals was integrated with phenol as internal standard. There was a sudden drop of D1 concentration (down to 42%) in the first 10 min, and then D1 decreased progressively over time. It should be noted that although the boiling point of D1 is high (125–130 °C at 2 torr),<sup>33</sup> a part of it may be lost in lyophilization by which D1 was isolated. This is why only 13% D1 was recovered at 70-min reaction time. Nevertheless, the NMR data show a reaction tendency similar to the HPLC results, confirming that the interfacial thiol-ene polymerization is a very fast process.

#### Encapsulation Efficiency and Stability of Microcapsules

In applications, one important performance parameter of microcapsules is their EE, which correlates closely to the diffusion property of shell materials. Thus, free oil that was not entrapped in microcapsules was extracted from the suspension using an organic solvent mixture, and EE was calculated using the following equation:

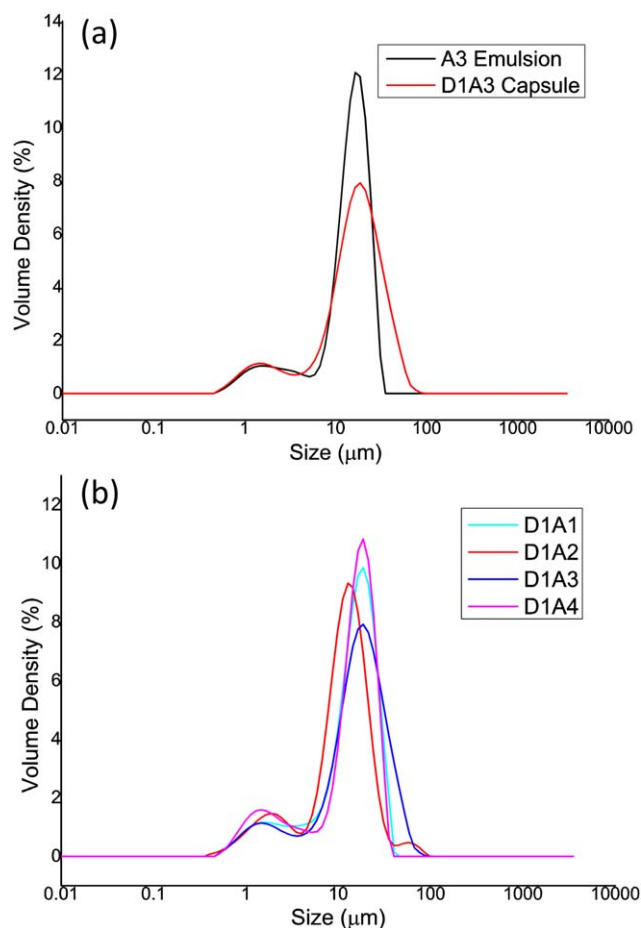


**Figure 2.** Particle size distributions of (a) A3 O/W emulsion and D1A3 microcapsule and (b) microcapsules D1A1–D1A4 as determined by light scattering. [Color figure can be viewed in the online issue, which is available at [wileyonlinelibrary.com](http://wileyonlinelibrary.com).]

$$EE (\%) = \frac{\text{Total amount of oil} - \text{Free oil}}{\text{Total amount of oil}} \times 100. \quad (1)$$

The results in Table I reveal that high EE was achieved in all microcapsules synthesized by interfacial thiol-ene polymerization: 91% (D1A3), 95% (D1A2), and 96% (D1A1 and D1A4). Considering that a small quantity of entrapped oil could be induced out of microcapsules during the extraction step, the actual EE might be even higher. To evaluate their stability, the microcapsules were stored in sealed vials at room temperature and 45 °C, and after 1 week and 1 month, EE was checked again. For D1A1 and D1A2, EE remained approximately unchanged during the 1-month storage period at both temperatures. The EE of D1A4, after 1 month, decreased from 96% to 92% at room temperature and to 86% at 45 °C, which is still acceptable. In comparison, although no floating oil was observed, the EE of D1A3 decreased from 91% to 83% at room temperature and 80% at 45 °C. The significantly lower initial EE of D1A3 and its lower stability on storage (especially at room temperature) indicate a looser and more permeable membrane structure, which might stem from the hydroxyl group in A3. Overall, except D1A3, the microcapsules showed high initial EE and the capability to resist excessive oil leakage for preventing phase separation and ensuring a constant release profile on application.

### Thermal Properties of Microcapsules

The release of fragrance from the microcapsules was examined using TGA. There were two weight loss regimes in the plots of TGA at 50 °C [Figure 4(a)]. The first stage was steep, corresponding to the evaporation of water and nonencapsulated fragrance. The second stage, starting from around 20% residual mass for D1A1–D1A2–D1A3, was very sluggish. This is because

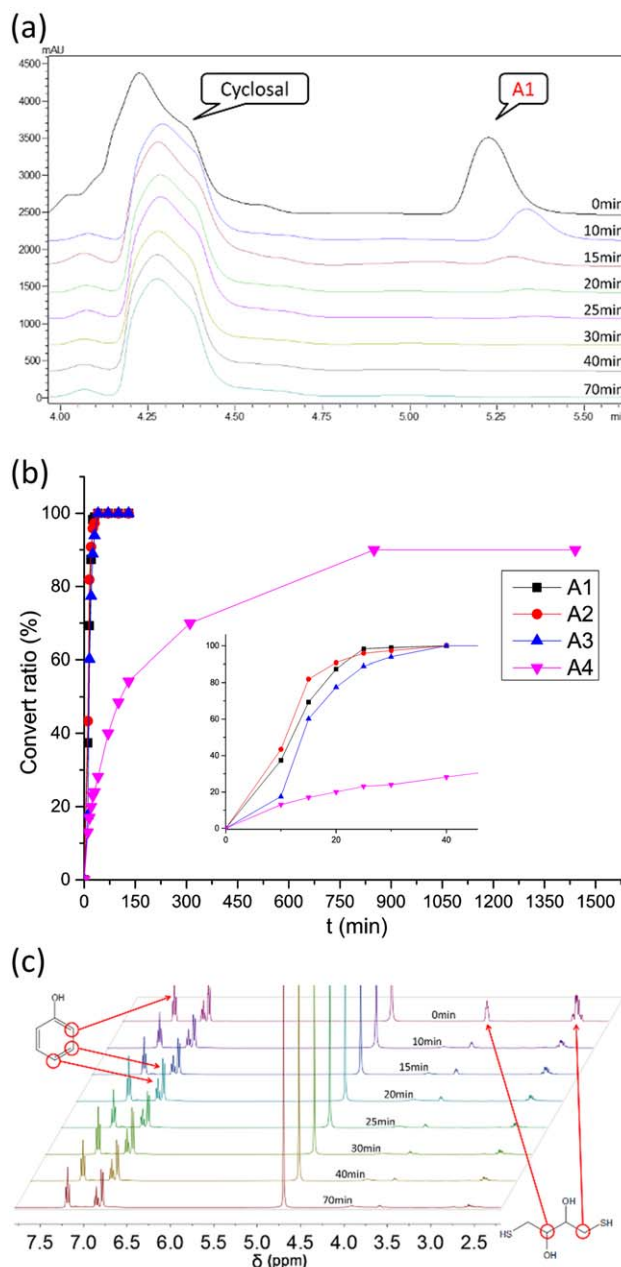


**Figure 3.** Kinetics of thiol-ene polymerization. (a) HPLC spectra of oil-soluble monomer A1 at set time intervals during the preparation of microcapsule D1A1. (b) Conversion ratios of A1–A4 followed over time and determined from HPLC data (0- to 40-min conversion ratios were magnified in the inset). (c)  $^1\text{H-NMR}$  spectra of water-soluble monomer D1 at set time intervals during the synthesis of microcapsule D1A1. [Color figure can be viewed in the online issue, which is available at [wileyonlinelibrary.com](http://wileyonlinelibrary.com).]

**Table I.** Encapsulation Efficiency (EE) of Microcapsules Prepared Using D1 and A1–A4 as the Monomers

Microcapsule	EE (%)	1 week EE (%) at room temperature	1 month EE (%) at room temperature	1 week EE (%) at 45 °C	1 month EE (%) at 45 °C
D1A1	96	96	95	95	94
D1A2	95	95	94	94	93
D1A3	91	86	83	82	80
D1A4	96	94	92	88	86

the membrane barrier dramatically slowed down the evaporation of encapsulated fragrance. The starting point at 20% residual mass is also close to the total percentage of oil loading, monomers, catalyst, and emulsifier in the formulation which equals to 23%. Microcapsule D1A4 seemed to be the most hermetic among the four samples synthesized; up to 67% encapsulated oil was retained by D1A4 after the 4-h incubation at 50 °C, whereas with D1A1–D1A2–D1A3, 52%, 51%, and 42% encapsulated oil was retained under the same condition. The lowest oil retention by D1A3 is in line with its lowest stability as evidenced by EE measurement during storage.

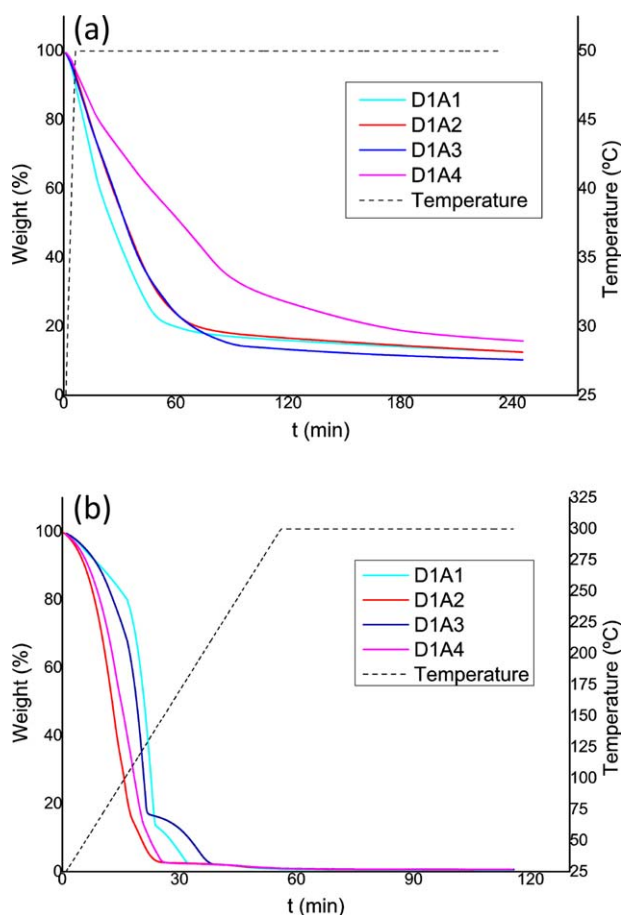


**Figure 4.** TGA curves of microcapsules D1A1–D1A4. (a) From room temperature to 50 °C at 5 °C/min and thermostat for 240 min. (b) From room temperature to 300 °C at 5 °C/min and thermostat for 60 min. [Color figure can be viewed in the online issue, which is available at [wileyonlinelibrary.com](http://wileyonlinelibrary.com).]

When the microcapsule suspension was heated to and held at 300 °C, which is higher than the boiling points of the fragrance components, all capsules were broken by overpressure generated, and the volatiles were completely released [Figure 4(b)]. Assuming 100% completion of the reaction of thiol group with acrylate group at 1/1 ratio, the polymeric shell material would comprise 0.96% mass of the final microcapsule suspension. If the polymeric shell is stable at 300 °C, and taking the catalyst  $K_2CO_3$  into account, there should be in total 1.02% mass retention. TGA results determined the final solid content of 0.53% (D1A1), 0.61% (D1A2), 0.68% (D1A3), and 0.65% (D1A4), obviously lower than the theory value. This gap was probably caused by the decomposition of smaller molecular weight species such as oligomers at high temperature.

## CONCLUSIONS

In conclusion, we have successfully developed a novel carrier system to encapsulate fragrance oil by interfacial thiol-ene polymerization. For all microcapsules synthesized, high EE ( $\geq 91\%$ ) of the model fragrance oil used was achieved with 0.96% shell materials for about 20% oil loading. Unlike conventional interfacial polymerization, the kinetic study showed that the interfacial thiol-ene polymerization is very rapid at room temperature: depending on the structure of the acrylate monomers, polymerization can be completed within 30 or 40 min, and the acrylate monomers were almost completely consumed in the presence of excess water-soluble monomer D1. Except D1A3, these microcapsules were stable at room temperature and 45 °C for 1 month. Therefore, the interfacial thiol-ene polymerization is demonstrated to be a facile and efficient approach to synthesize new and performing shell materials for fragrance microencapsulation. We expect that this approach can be extrapolated to other fields of application such as controlled drug delivery.

## ACKNOWLEDGMENTS

The authors thank the support by Shanghai Pujiang Talent Program (No. 14PJ1433300) from the Shanghai Science and Technology Committee. The authors also thank Arnaud Struillou for valuable discussions and Fan Zhang for the assistance in size measurement.

## REFERENCES

1. Beerling, J. In *The Chemistry of Fragrances: From Perfumer to Consumer*; Sell, C. S., Ed.; The Royal Society of Chemistry: Cambridge, UK, 2006; Chapter 9, pp 168–183.

2. Winkel, C. In *Chemistry and Technology of Flavors and Fragrances*; Rowe, D. J., Ed.; Blackwell Publishing: Oxford, UK, **2005**; Chapter 10, pp 244–260.
3. Tekin, R.; Bac, N.; Erdogmus, H. *Macromol. Symp.* **2013**, *333*, 35.
4. He, Y.; Bowen, J.; Andrews, J. W.; Liu, M.; Smets, J.; Zhang, Z. *J. Microencapsul.* **2014**, *31*, 430.
5. Holzner, G.; Verhovnik, G. (to Firmenich SA). WO Pat. 2,006,018,694, February 23 (**2006**).
6. Chen, H.; Jones, C. C.; Pan, X.; Wang, J. (to Hindustan Unilever Ltd.). WO Patent 2,013,026,657, February 28 (**2013**).
7. Arshady, R. *J. Microencapsul.* **1989**, *6*, 13.
8. Zhang, Y.; Rochefort, D. *J. Microencapsul.* **2012**, *29*, 636.
9. Ouali, L.; Benczedi, D. (to Firmenich SA). U.S. Pat. 20,080,206,291, August 28 (**2008**).
10. Pichon, N.; Godefroy, S.; Struillou, A. (to Firmenich SA). WO Pat. 2,013,092,375, June 27 (**2013**).
11. Lei, Y.; Xu, L.; Joyce, C. (to International Flavors & Fragrances, Inc.). U.S. Pat. 20,130,337,023, December 19 (**2013**).
12. Rodrigues, S. N.; Martins, I. M.; Fernandes, I. P.; Gomesa, P. B.; Mata, V. G.; Barreiro, M. F.; Rodrigues, A. E. *Chem. Eng. J.* **2009**, *149*, 463.
13. Jacquemond, M.; Jeckelmann, N.; Ouali, L.; Haefliger, O. P. *J. Appl. Polym. Sci.* **2009**, *114*, 3074.
14. Kolb, H. C.; Finn, M. G.; Sharpless, K. B. *Angew. Chem. Int. Ed. Engl.* **2001**, *40*, 2004.
15. Lutz, J. F. *Angew. Chem. Int. Ed. Engl.* **2007**, *46*, 1018.
16. Qin, A.; Lam, J. W. Y.; Tang, B. Z. *Macromolecules* **2010**, *43*, 8693.
17. Golas, P. L.; Matyjaszewski, K. *Chem. Soc. Rev.* **2010**, *39*, 1338.
18. Hoyle, C. E.; Lowe, A. B.; Bowman, C. N. *Chem. Soc. Rev.* **2010**, *39*, 1355.
19. Lowe, A. B. *J. Polym. Sci. Part A: Polym. Chem.* **2010**, *1*, 17.
20. Lowe, A. B. *Polymer* **2014**, *55*, 5517.
21. De Geest, B. G.; Camp, W. V.; Du Prez, F. E.; De Smedt, S. C.; Demeester, J.; Hennink, W. E. *Chem. Commun.* **2008**, *44*, 190.
22. Zhang, J.; Li, C.; Wang, Y.; Zhuo, R. X.; Zhang, X. Z. *Chem. Commun.* **2011**, *47*, 4457.
23. Zhang, J.; Xu, X. D.; Liu, Y.; Liu, C. W.; Chen, X. H.; Li, C.; Zhuo, R. X.; Zhang, X. Z. *Adv. Funct. Mater.* **2012**, *22*, 1704.
24. Roux, R.; Sallet, L.; Alcouffe, P.; Chambert, S.; Sintesz-Zydowicz, N.; Fleury, E.; Bernard, J. *ACS Macro Lett.* **2012**, *1*, 1074.
25. Siebert, J. M.; Baier, G.; Musyanovych, A.; Landfester, K. *Chem. Commun.* **2012**, *48*, 5470.
26. Huang, C. J.; Chang, F. C. *Macromolecules* **2009**, *42*, 5155.
27. Ochs, C. J.; Such, G. K.; Yan, Y.; Van Koeverden, M. P.; Caruso, F. *ACS Nano* **2010**, *4*, 1653.
28. Liang, K.; Such, G. K.; Zhu, Z.; Yan, Y.; Lomas, H.; Caruso, F. *Adv. Mater.* **2011**, *23*, H273.
29. Such, G. K.; Gunawan, S. T.; Liang, K.; Caruso, F. *Macromol. Rapid Commun.* **2013**, *34*, 894.
30. Zou, J.; Hew, C. C.; Themistou, E.; Li, Y.; Chen, C. K.; Alexandridis, P.; Cheng, C. *Adv. Mater.* **2011**, *23*, 4274.
31. Paret, N.; Trachsel, A.; Berthier, D. L.; Herrmann, A. *Angew. Chem. Int. Ed. Engl.* **2015**, *54*, 2275.
32. Dhumal, S. S.; Wagh, S. J.; Suresh, A. K. *J. Membr. Sci.* **2008**, *325*, 758.
33. Evans, R. M.; Fraser, J. B.; Owen, L. N. *J. Chem. Soc.* **1949**, 248.